Lawrence Berkeley National Laboratory
LBL Publications

Title

WATER ADSORPTION ON THE (001) PLANE OF Fe2O3: AN XPS, UPS, AES AND TPD STUDY

Permalink

https://escholarship.org/uc/item/6fr0v51j

Authors

Hendewerk, M.
Salmeron, M.
Somorjai, G.A.

Publication Date

1985-11-01

Lawrence Berkeley Laboratory
UNIVERSITY OF CALIFORNIA

Materials & Molecular Research Division

WATER ADSORPTION ON THE (001) PLANE OF
Fe₂O₃: AN XPS, UPS, AES AND TPD STUDY

M. Hendewerk, M. Salmeron, and G.A. Somorjai

November 1985

DISCLAIMER

WATER ADSORPTION ON THE (001) PLANE OF

Fe_2O_3: AN XPS, UPS, AES AND TPD STUDY

By

M. Hendewerk, M. Salmeron* and G.A. Somorjai

Materials and Molecular Research Division
*Center for Advanced Materials
Lawrence Berkeley Laboratory 862-203
Berkeley, California 94720

ABSTRACT:

The adsorption of H_2O on the (001) plane of the corundum phase of Fe_2O_3 was studied by XPS, UPS, Auger and TPD. On the stoichiometric surface only ice condensation was observed below 200 K. Oxygen-deficient surfaces were prepared by Ar bombardment. This process gives rise to a decrease in work function up to 1 eV. On these surfaces H_2O decomposed to form OH that decomposed at higher temperatures to produce H_2. If the bombarded surface was previously annealed above 475 K, no H_2 evolution was observed. This result coupled with the observed increase in work function indicates that annealing removes the Fe^{+2} species from the outermost layer, however they are still clearly visible by XPS and UPS in the subsurface region.

1. INTRODUCTION:

Iron oxide (Fe_2O_3) has been investigated as a photoelectrode for the photodissociation of H_2O (1-3). This interest is due to both its convenient band gap, around 2 eV, that matches the solar spectrum and to its corrosion resistance in aqueous basic solutions.

Electrochemical studies have shown the importance of surface effects in the Fe_2O_3 photoelectrodes. These effects include the presence of surface states, adsorbed species, and the electronic structure that controls the transport of electrons to and from the surface (4-8). In spite of these findings there have been very few atomic and spectroscopic studies of the surface properties of this material. Therefore we have undertaken studies of the surface properties of single crystals of Fe_2O_3 in Ultra High Vacuum, with several surface sensitive spectroscopic techniques. These include Low Energy Electron Diffraction (LEED), X-ray and Ultraviolet Photoelectron Spectroscopies (XPS and UPS), Auger Spectroscopy and Thermal Programmed Desorption (TPD).

With these techniques we investigated the adsorption of H_2O on both the clean stoichiometric (001) basal plane of the corundum structure of Fe_2O_3 and on the oxygen deficient surface prepared by Argon ion sputtering.

We found that strong chemisorption of H_2O occurs only when Fe^{+2} species are present in the outermost atomic plane. We found also that these reduced surface species are rapidly removed from the top surface layer by heating above 475 K. The Fe^{+2} species are then present in shallow subsurface layers and remain there stable at temperatures up to 775 K for long periods of time (30 minutes of longer).

Finally, the effect of adsorbed potassium was also investigated. Its main effect is to decompose H_2O to form probably KOH that in turn decomposes thermally to give H_2 evolution.

II. EXPERIMENTAL:

The experiments were conducted on Ge-doped Fe_2O_3 single crystals grown in our laboratory by CVD as described elsewhere (9). The crystal orientation is the (001) basal plane of the corundum structure. The crystals show readily the hexagonal LEED patterns after evacuation of the chamber without any treatment (10). The bulk properties of these Ge-doped crystals have been determined and shown to be identical to those of pure Fe_2O_3 including the band gap and electrochemical properties (9). The conductivity of these doped crystals, however, is much higher (1 Ohm x cm) than that of pure Fe_2O_3 (10^6 Ohm x cm), which is advantageous for studies using electron spectroscopies.

The Ultrahigh Vacuum studies were carried out in a stainless steel chamber with a base pressure of 2×10^{-10} torr. Standard Physical Electronics equipment was used for Auger, UPS, XPS and LEED. The chamber is also equipped with a Quadrupole Mass Spectrometer and a He discharge source for UPS studies. The XPS spectra were obtained using a Mg Kα X-ray source. Peak positions were calibrated by setting the C 1s signal to 284.5 eV.

The crystal was biased during UPS scans in order to observe clearly the secondary electron emission onset. The work function of the spectrometer was assumed to be constant, so that changes in the work function of the sample were obtained from the shift in the onset of the secondary electron emission.

TPD spectra were obtained with the ionizer of the mass spectrometer encapsulated except for a protruding 1 mm aperture. Water exposures were measured in Langmuirs ($1L=10^{-6}$ torr x sec.) without correction for ion gauge sensitivity changes.

The single crystal platelets were a few tenths of a mm thick and were mounted by melting a very small quantity of In on a Ta foil, smaller than the crystal size, and placing the crystal on the In, that acted as a glue. The surface tension of the In above its melting point (429 K) was sufficient to support the vertically mounted crystals even at 1300 K. The temperature was measured with a chromel-alumel thermocouple spot-welded directly to the Ta foil. Because of the thinness of the platelets, the temperature of the foil and the crystal were assumed to be identical. The phase transition from Fe_2O_3 to Fe_3O_4

occurs at 1350 K so that no attempts were made to heat above 1300 K. No In was observed by Auger or XPS to have diffused to the front face of the crystal, even after heating to 1300 K, although we were careful to avoid such high temperatures for more than a few seconds at a time. The sample was cooled by thermal transport from the Ta supports to a liquid nitrogen reservoir down to 120 K.

III.   RESULTS AND DISCUSSION:

III.I H_2O adsorption on stoichiometric Fe_2O_3-(001)

The inertness of the basal plane of Fe_2O_3 that is apparent from the observation of its LEED pattern directly after evacuation form air (10), is again manifested in its H_2O adsorption properties. Only low temperatur? physisorption was observed as shown in the TPD spectra of Fig. 1. The peak of H_2O is observed at temperatures shifting from 175 K to 200 K as the exposure increases from 1.5 to 80 Langmuirs. This observation and the fast fall-off at the high temperature edge are all indicative of zero order kinetics. The activation energy for desorption was calculated to be 11.8 Kcal/mol, which is close to the sublimation heat of ice (12.2 Kcal/mol). These results indicate that water forms ice clusters on the (001) plane of Fe_2O_3, with very little chemical interaction with the substrate. The UPS results shown in Fig. 2 confirm these observations.

After water adsorption at 120 K, the UPS curves show the presence of water induced features (Fig. 2 bottom curve). Only the peaks due to the lb_1 and $3a_1$ molecular orbitals are observed clearly. The lb_2 peak is obscured by the secondary electron peak. UPS curves from multilayers of

ice show the three peaks clearly (see Fig. 9, bottom curve). After heating to 190 K we observe the disappearance of all the water features in accordance with the TPD results.

III.2   Sputtered Fe_2O_3

III.2.1 Work function changes

A more reactive surface can be prepared by introducing surface defects like O-vacancies through Ar ion sputtering. Three different experiments were performed to characterize the defective surface. In the first one we measured the change in the work function $\Delta\Phi$ as a function of sputtering time. The results for a 3 µA, 500 eV Ar+ beam are shown in Fig. 3. A continuous decrease in Φ is observed until a saturation is reached. The total change in the work function was found to vary between 0.8 and 1 eV in different experiments. Since the basal plane contains oxygen ions only, the initial sputtering removes oxygen preferentially and thereby second layer Fe atoms are exposed. This process creates dipoles with the opposite orientation to the initial ones and explains the observed decrease in work function. As the bombardment proceeds, second, third and deeper layers are affected probably in a disordered way, until a steady state is reached where the ratio of dipoles of both orientations remains constant. For a 500 eV Ar ion beam this process takes 9 minutes at 3 µA as shown in Fig. 3.

Annealing the bombarded surface to various temperatures causes the work function to increase in the manner shown in Fig. 4. As can be seen,

the work function of the initial unperturbed surface is not recovered even for temperatures as high as 775 K.

A rapid initial increase is observed for temperatures of 475 K and above, followed by a very slow increase with annealing time. The initial increase of Φ becomes slower below 475 K as shown in the figure. We interpret these results as due to a rapid exchange between surface oxygen vacancies and bulk oxygen. The diffusion of bulk O-vacancies after this initial process, has probably a much higher activation energy. As seen in the figure, the value of Φ after the initial change, was stable for periods of 30 minutes at least. The crystal surface was restored to its initial stoichiometric condition by heating to 600 K in 5×10^{-6} torr of O_2.

III.2.2 UPS and XPS measurements

As found also by other authors (11,12), Ar^+ sputtering creates reduced Fe species that give rise to emission from states above the valence band, i.e. within the gap. This is shown in the UPS spectrum of Fig. 5, where a shoulder above the conduction band is observed to increase in intensity with sputtering time until it saturates.

The difference between the energies of the leading edges before and after sputtering is approximately 2 eV, i.e. the band gap energy. The iron species responsible for this emission could be either Fe^o in small metallic clusters, or Fe^{+2} in various local O-vacancy configurations.

We performed then a series of XPS measurements to investigate the oxidation state of iron. In the results shown in Fig. 6, we compare the $2P_{3/2}$-$2P_{1/2}$ spectral region of sputtered Fe_2O_3 to that of the stoichiometric oxide and of clean Fe metal. These spectra show that the sputtered surface contains very little Fe°. Most of the reduced iron is in the Fe^{+2} formal oxidation state. The relative position of the $2P_{3/2}$ line for Fe^{+2} as found by other authors (13-16) is shown by the vertical lines.

Heating the surface to various temperatures (up to 750 K) for up to 30 min. did not change appreciably the UPS and XPS spectra, indicating that the reduced iron species are still present in the first few layers below the surface.

III.2.3 H_2O adsorption on sputtered Fe_2O_3

The TPD spectra of H_2O adsorbed on the sputtered surface are shown in Fig. 7. We observe that the molecular water spectrum is similar to that of the stoichiometric surface. Both the temperature range (around 190 K) and the shift towards higher temperatures as the coverage increases, indicate the formation of weakly bound ice particles. There are, however, a number of differences. At low exposures, two peaks are observed at approximately 175 K and 200 K. The first one grows with exposure and shifts to higher temperatures while the second one saturates after a short exposure. In addition, the TPD peaks are wider than in the stoichiometric surface.

We could interpret the low exposure 200 K peak as due to the formation of two-dimensional ice bilayer islands that form on the more reduced patches of the surface as observed in the case of metallic substrates (17-19).

The increased width of the peaks could be due to a wider range of ice island sizes or to a larger variation in the H-bonding energies in the ice clusters induced by the more heterogeneous substrate.

The most important difference with respect to the stoichiometric surface, however, is the observation of H_2 evolution in a broad peak, ranging from 220 K to 750 K, as shown in Fig. 8.

H_2 evolution, however, was observed only on freshly sputtered surfaces that had not been annealed above 475 K. If the surface is annealed to this temperature and above, no H_2 evolution is observed.

It appears then, that only the Fe^{+2} species in the outermost atomic plane, can adsorb water strongly. Subsurface Fe^{+2} species, although stable, are not contributing to the chemisorption of H_2O.

To further confirm this point we studied the evolution of the UPS spectra of H_2O adsorbed on the sputtered surface as a function of temperature. The spectra are shown in Fig. 9, along with spectra before H_2O adsorption and after multilayer adsorption. The three prominent features due to the $1b_2$, $3a_1$, and $1b_1$ molecular orbitals of water clearly dominate the pphotoelectron spectrum of the ice multilayers. The

thickness of the ice film must be at least 20 Å to completely suppress the underlaying Fe_2O_3 spectrum. We observe also, that the peak at approximately 10 eV binding energy is present above 200 K and up to 370 K. After the desorption of the molecular water at 190 K, this peak shifts to higher binding energies by roughly 0.5 eV. This result seems to indicate that OH species are now present in the surface. Similar shifts in going from H_2O to OH have been observed by other authors (19-20).

III.2.4 K and H_2O adsorption on Fe_2O_3

Potassium was deposited on the surface of the crystal via a K source heated by a DC power supply. Coverages were monitored by the Auger peak to peak ratios of the K(252) to Fe(651) transitions. It was possible to deposit multilayers of K up to K/Fe ratio of 36. These layers, however, were easily desorbed upon heating to 600 K approximately as shown in Fig. 10. After the desorption of the multilayers the remaining K, with a ratio K/Fe=5 to 6, could not be removed by heating. It was readily removed, however, by sputtering. This is possibly indicative of compound formation between the K and the Fe_2O_3. This result is in contrast with the behaviour of K overlayers on oxidized Fe(100), where other authors observed complete removal of K in the range between 550 K and 700 K (13).

The coadsorption of water and K on iron oxide was also studied. At 120 K the crystal was first sputtered to produce the O-vacancy defect sites, and then the K was adsorbed with a coverage below the monolayer (K/Fe=1).

The TPD spectrum showed only one low temperature molecular H_2O peak (as in Fig. 7), and two broad H_2 peaks, one at 260 K and one at 410 K as can be seen in Fig. 8. The broad peak at 410 K is similar to the H_2 peak observed in the sputtered crystal without K adsorbed on the surface. The low temperature peak can then be appropriately assigned to the desorption of H_2 from a K complex, most likely KOH, as it decomposes. This is supported by the Auger data. The K/Fe ratio remains the same before and after the TPD.

IV.   CONCLUSIONS:

The results of our study can thus be summarized as follows:

1. The basal plane of the corundum structure of Fe_2O_3 is extremely inert. Water physisorbs only as ice at low temperatures and desorbs in the range of 175 to 200 K.

2. Ar^+ ion sputtering produces O-vacancies that expose mostly Fe^{+2} species and lower the work function of the surface.

3. Surface Fe^{+2} species are very unstable and disappear into the subsurface layers rapidly upon heating above 275 K. The subsurface Fe^{+2} species are stable at temperatures up to 775 K, for extended periods of time (>30 min.).

4. Only surface Fe^{+2} species chemisorb H_2O strongly to produce OH species that decompose to give H_2 upon heating.

5. K binds strongly to the (001) surface plane of Fe_2O_3 in the monolayer range. K multilayers desorb easily above 600 K. With H_2O it forms a compound (probably KOH) that decomposes at 275 K and above to give H_2 and a surface K/Fe_2O_3 compound.

ACKNOWLEDGMENTS:

References:

1. K.L. Hardee and A.J. Bard, J. Electrochem. Soc., 123, 1024 (1976).

2. R.K. Quinn, R.D. Nasby and R.J. Baughman, Mat. Res. Bull. 11, 1011 (1976).

3. G.A. Somorjai, M. Hendewerk and J.E. Turner, Catal. Rev. Sci. Eng. 26, 683 (1984).

4. J.H. Kennedy and K.W. Frese, Jr., J. Electrochem. Soc., 125, 723 (1978).

5. M. Anderman and J.H. Kennedy, J. Electrochem. Soc., 131, 21 (1984).

6. H. Gerischer, in "Photoelectrochemistry, Photocatalysis and Photoreactors", NATO Advanced Science Study Institute, series C, Vol. 149, p. 39. Edited by M. Schiavello, Erice, Trapani, Italy, 1984, p. 39.

7. R. Memming, Ibid., p. 107.

8. J.B. Goodenough, Ibid., p. 155.

9. K. Sieber, C. Sanchez, J.E. Turner and G.A. Somorjai, J. Chem. Soc. Faraday Trans. (in press 1985).

10. C. Sanchez, M. Hendewerk, K.D. Sieher and G.A. Somorjai, J. Solid State Chem. (in prerss 1985).

11. Lin Zhang-da, Cheng Yun-qi, Wu Shu-yao, Qi Shang-xue and Xie Kai, Chinese Physics 4,325 (1984).

12. R.L. Kurtz and V.E. Henrich, Surf. Sci. 129, 345 (1983).

13. S.R. Kelemen, A. Kaldor and D.J. Dwyer, Surf. Sci. 121, 45 (1982).

14. C.R. Brundle, T.J. Chuang and K. Wandelt, Surf. Sci. 68, 459 (1977).

15. G.C. Allen, M.T. Curtis, A.J. Hooper and P.M. Tucker, J. Chem. Soc. Dalton Trans., 1525 (1974).

16. P.D. Schulze, T.E. Neil, S.L. Shaffer, R.W. Smith and D.S. McKay, J. Vac. Sci. Technol. (A), 3, 6 (1985).

17. H. Ibach and S. Lehwald, Surf. Sci. 91, 187 (1980).

18. G.B. Fischer and J.L. Gland, Surf. Sci. 94, 446 (1980).

19. G.B. Fischer and B.A. Sexton, Phys. Rev. Letters, 44, 683 (1980).

20. D.J. Dwyer, S.R. Kelemen and A. Kaldor, J. Chem. Phys. 76, 1832 (1982).

FIGURE CAPTIONS

Fig. 1   Thermal programmed desorption of H_2O adsorbed on the (001) basal plane of Fe_2O_3. Exposures are indicated in Langmuirs ($1L=10^{-6}$ torr x sec.).

Fig. 2   Ultraviolet photoelection spectra (HeI, $h\nu = 21.2$ eV) from H_2O adsorbed on Fe_2O_3 - (001) after heating to the indicated temperature. The position of the peaks induced by the three molecular orbitals of H_2O in ice as found in Fig. 9 are also shown.

Fig. 3   Work function change of Fe_2O_3 as a function of Ar sputtering time.

Fig. 4   Work function change of the sputtered Fe_2O_3 (at saturation dose) as a function of annealing time for various temperatures.

Fig. 5   Evolution of the photoelectron spectra of Fe_2O_3-(001) as a function of sputtering time. Notice the appearance of the shoulder near zero binding energy due to reduced iron.

Fig. 6   X-ray photoelectron spectra of the $2P_{3/2}-2P_{1/2}$ core levels for stoichiometric Fe_2O_3, sputtered Fe_2O_3 and a clean Fe foil. The three vertical lines show the relative peak position for Fe^{+2} species as found by several authors (13-16).

Fig. 7   Thermal programmed desorption of H_2O adsorbed on the sputtered Fe_2O_3-(001) plane. Exposures are indicated in Langmuirs.

Fig. 8   Thermal programmed desorption of H_2 from adsorbed H_2O on the sputtered Fe_2O_3 (dashed line), and on the same surface with a submonolayer amount of preadsorbed potassium.

Fig. 9   Ultraviolet photoelectron spectra (HeI, $h\nu = 21.2$ eV), from H_2O adsorbed on the sputtered Fe_2O_3-(001) plane. Above 190 K the peak due to the $3a_1$ molecular orbital appears at ≈ 0.5 eV higher binding energy, indicating the presence of OH species.

Fig. 10 Auger peak ratio of potassium and iron as a function of temperature. Multilayers of K are present below 600 K approximately.
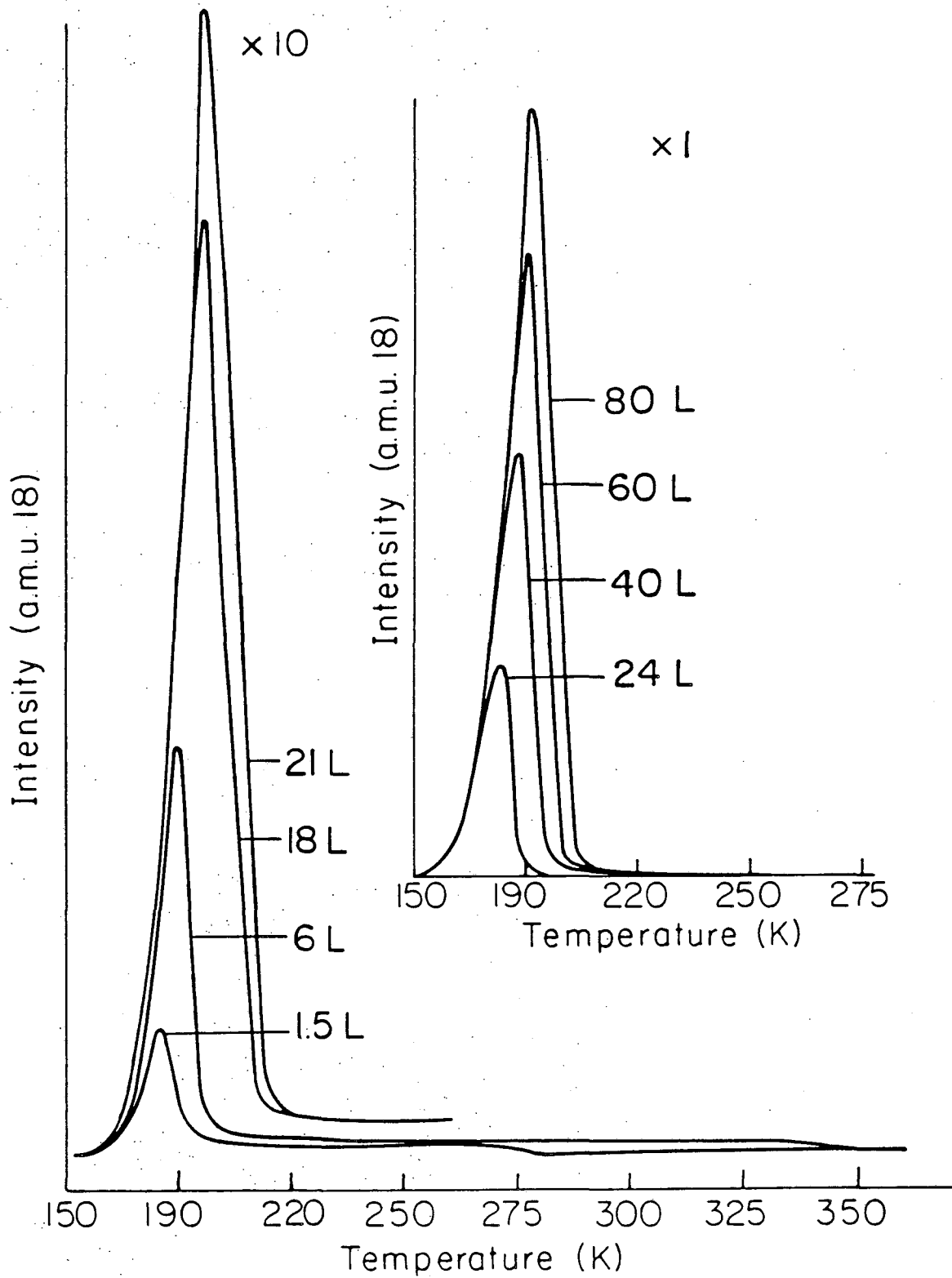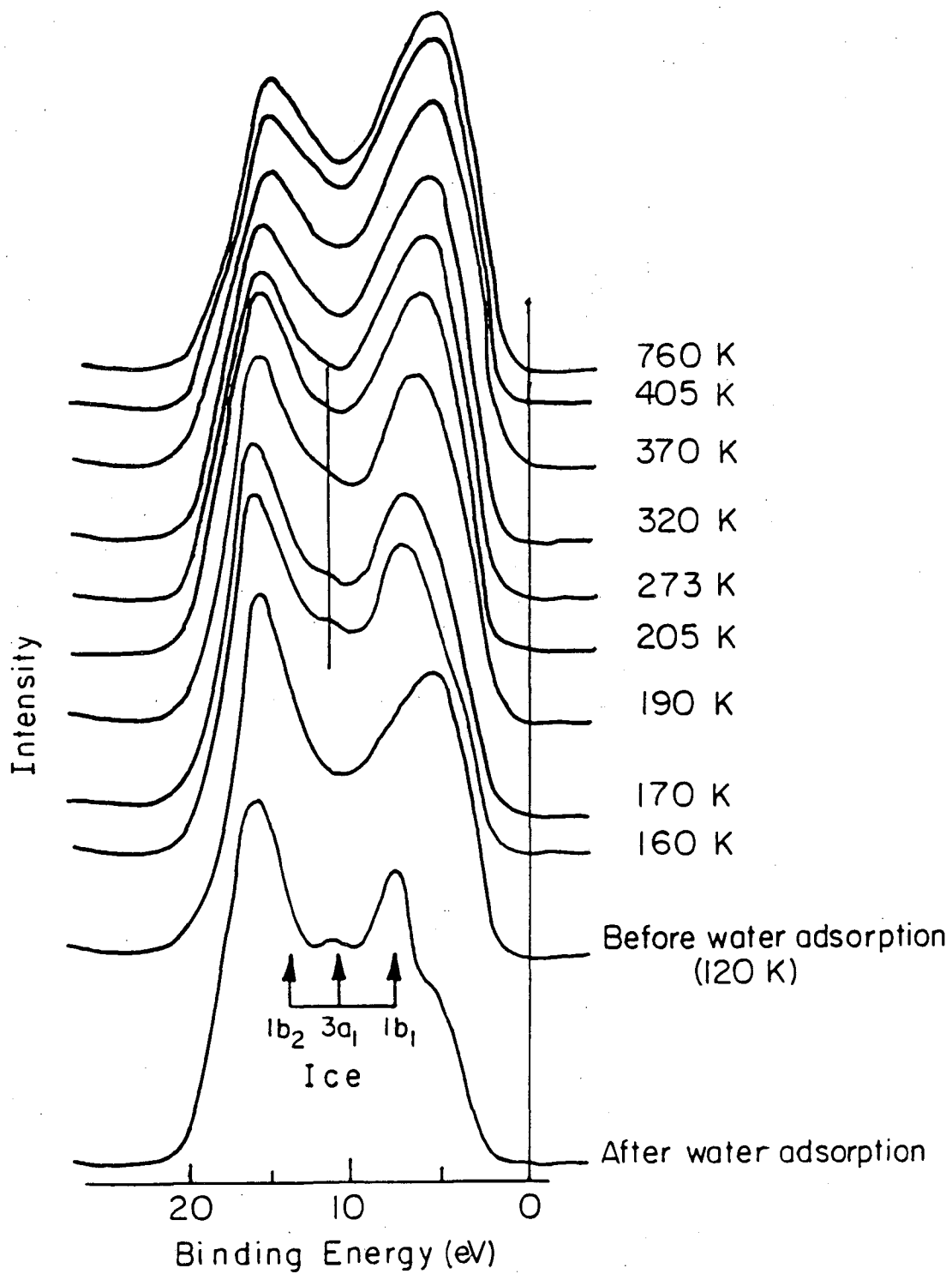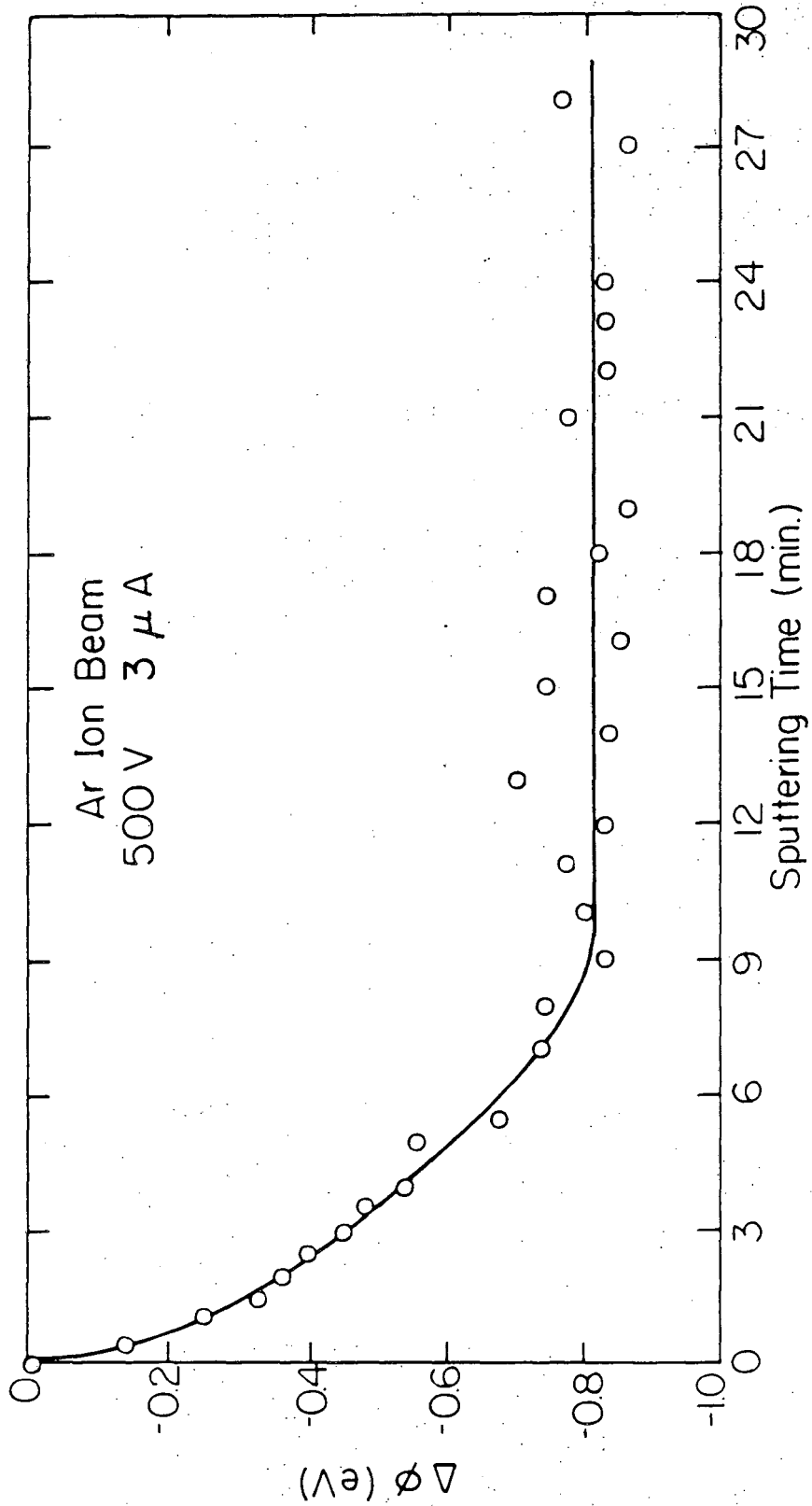
Fig. 1.

XBL 856-6297

Fig. 2.

XBL 8511-4508

Ar Ion Beam
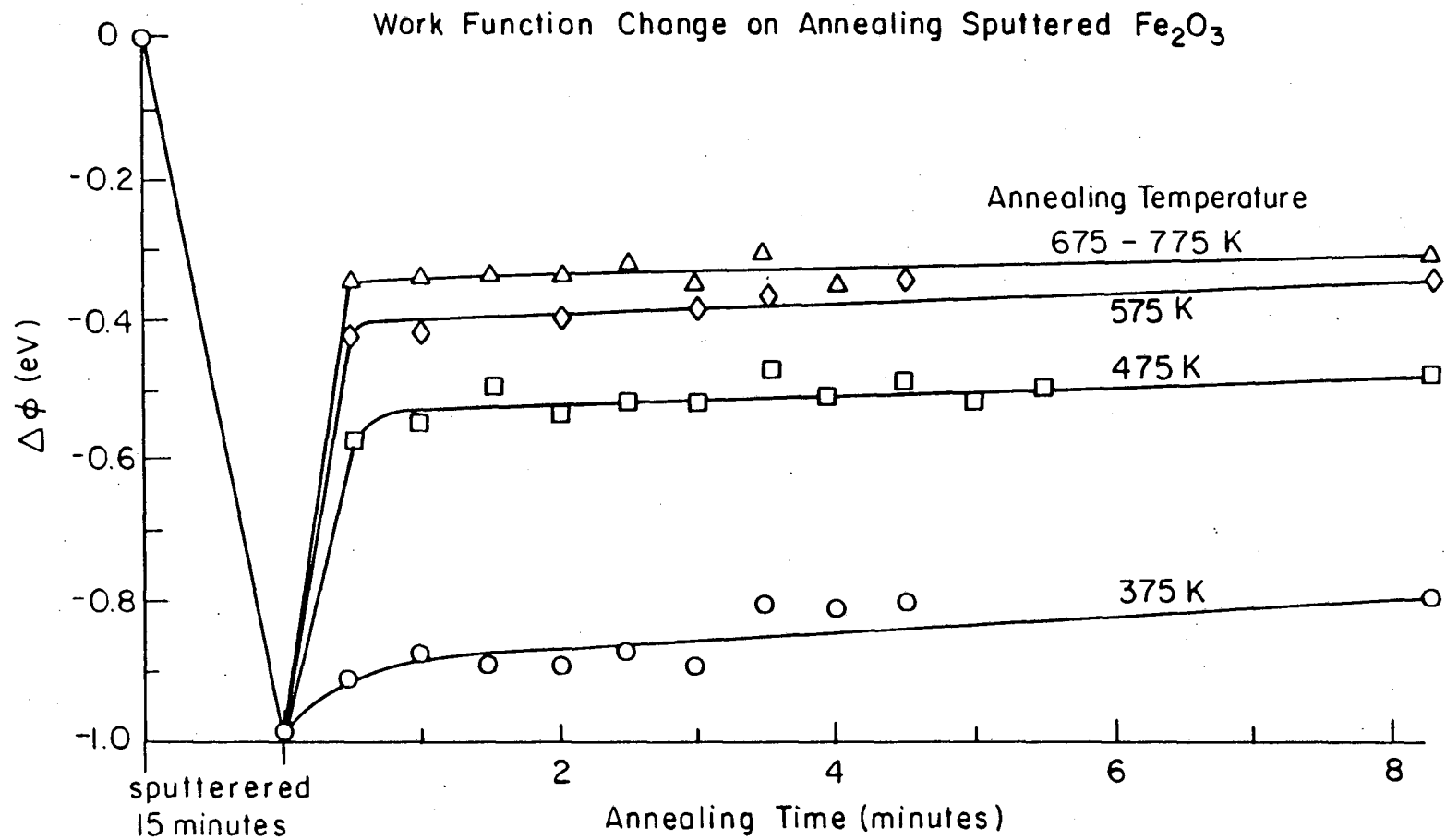500 V 3 μA

Sputtering Time (min.)
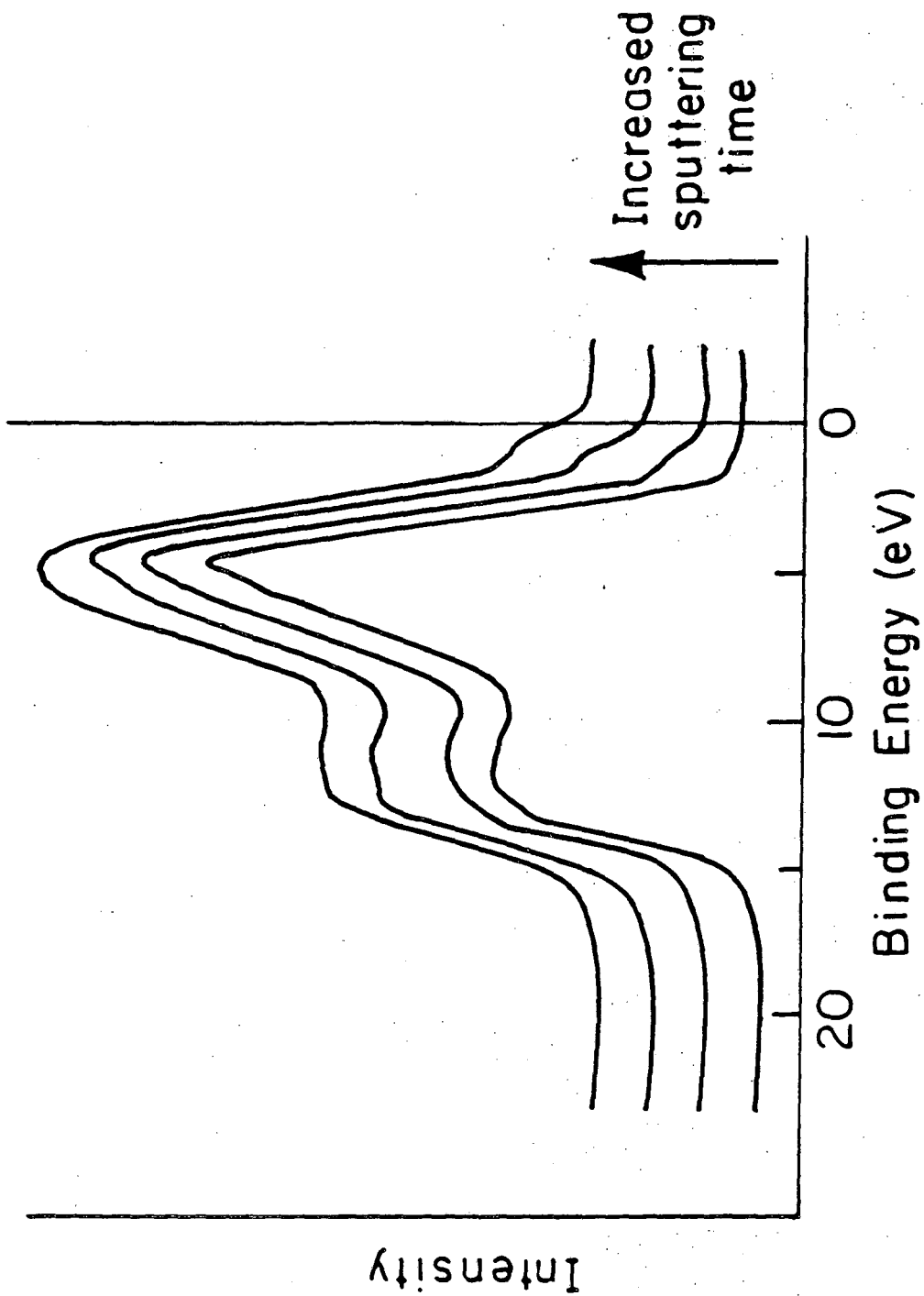
Δφ (eV)

Fig. 3.

XBL 856-6302

Fig. 4.

Fig. 5.

XBL 8511-4507

X-ray Photoelectron Spectra
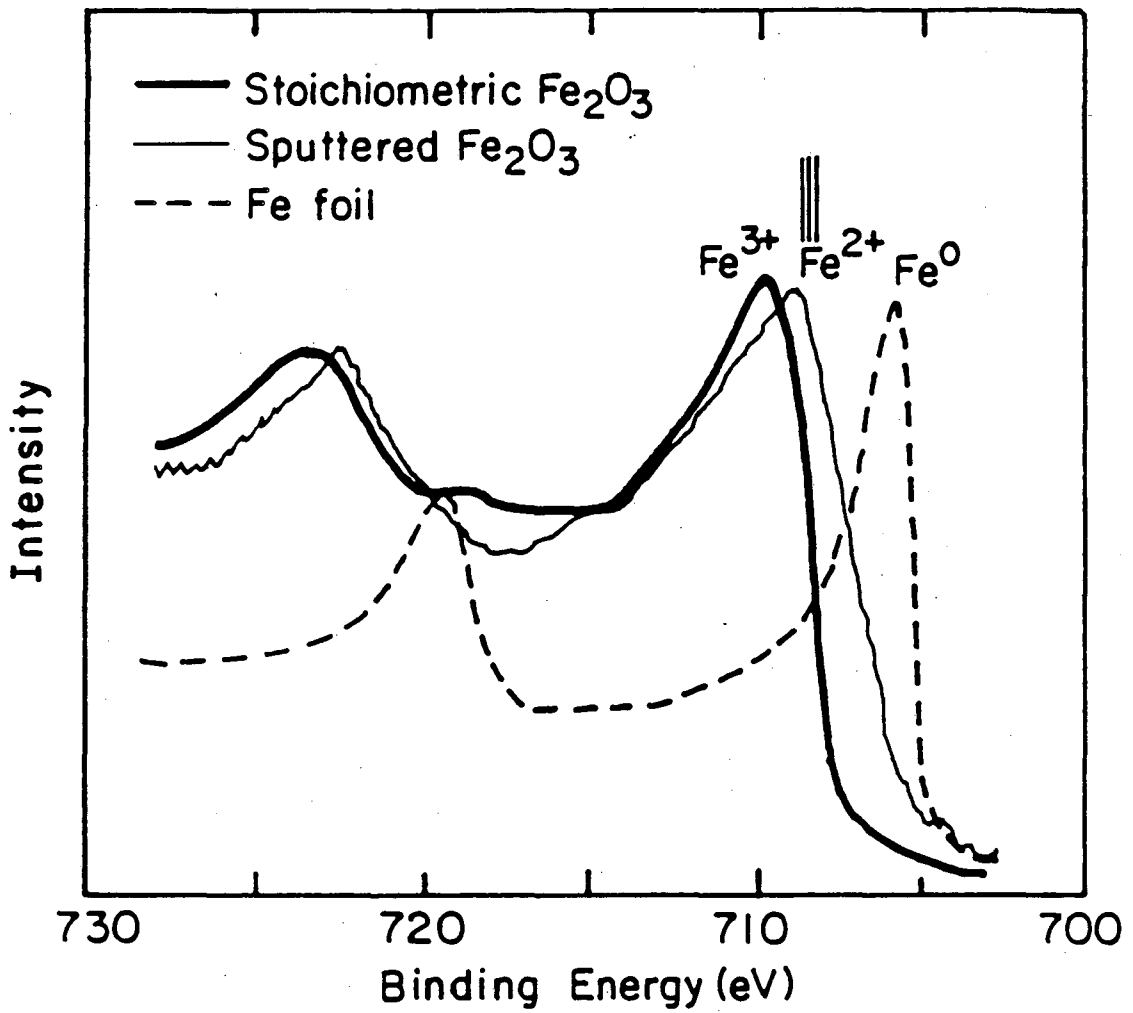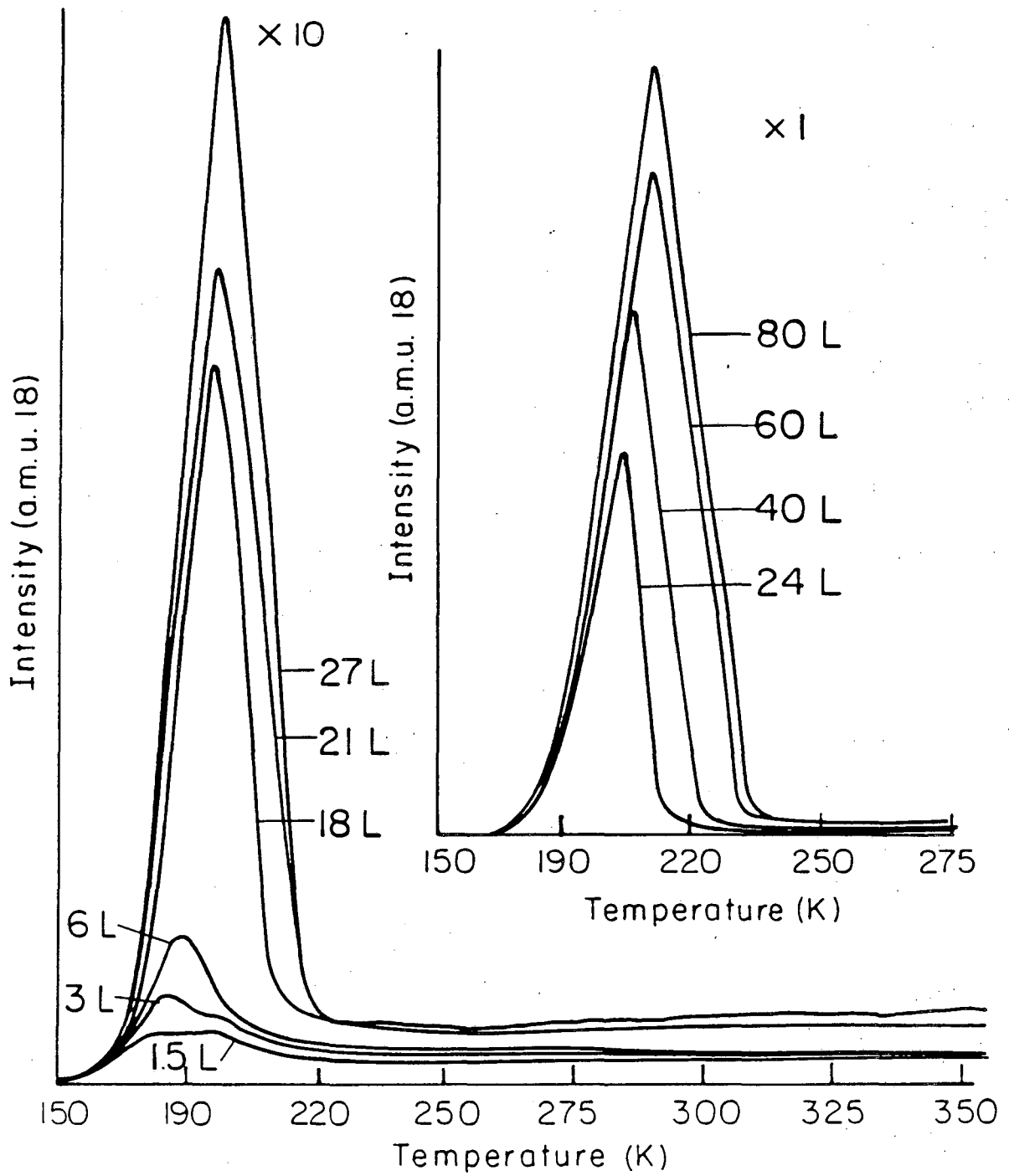

Fig. 6.   XBL 856-6296

Fig. 7.

XBL 856-6298
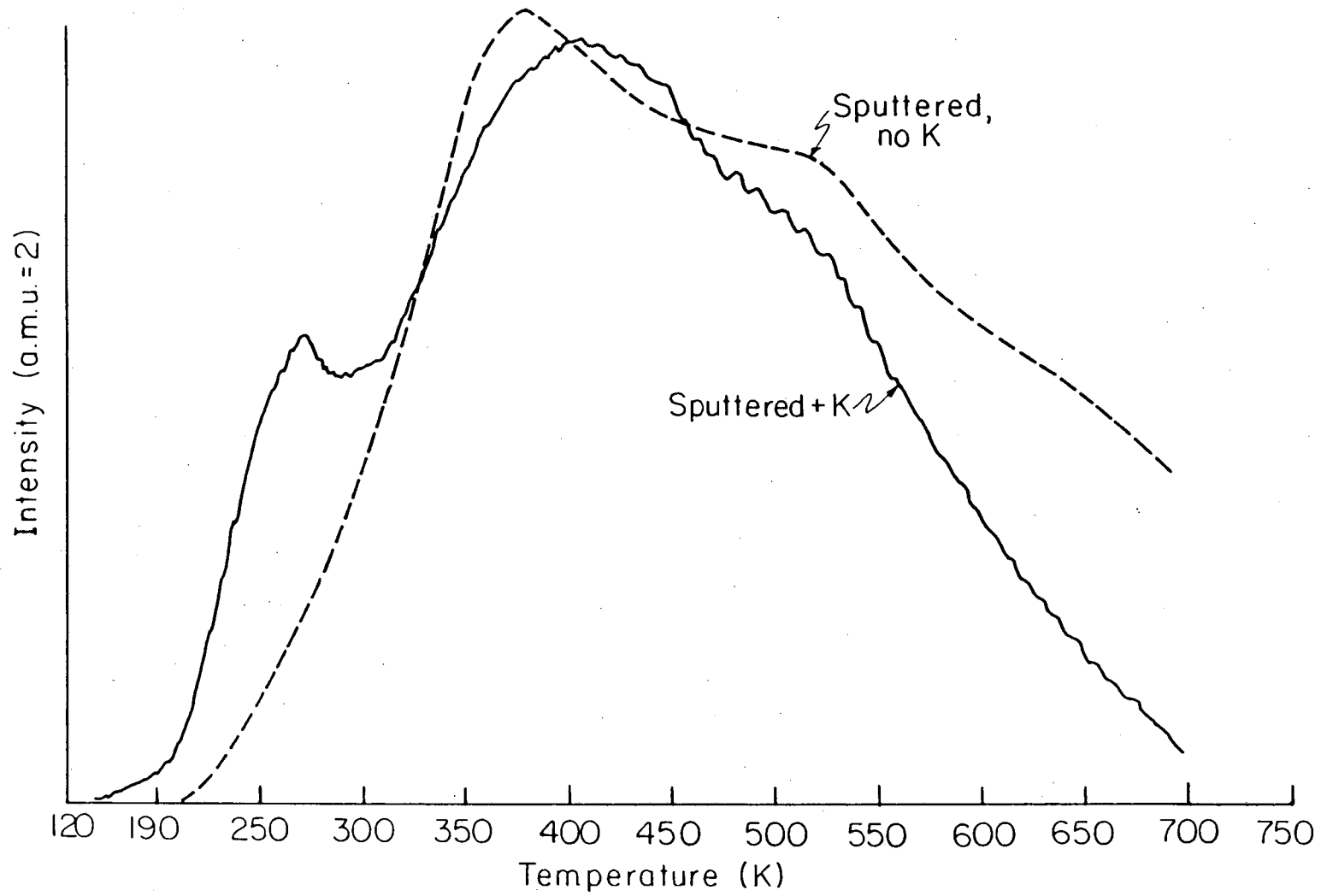
Fig. 8:

XBL 856-6300

Fig. 9.

XBL 856-6303
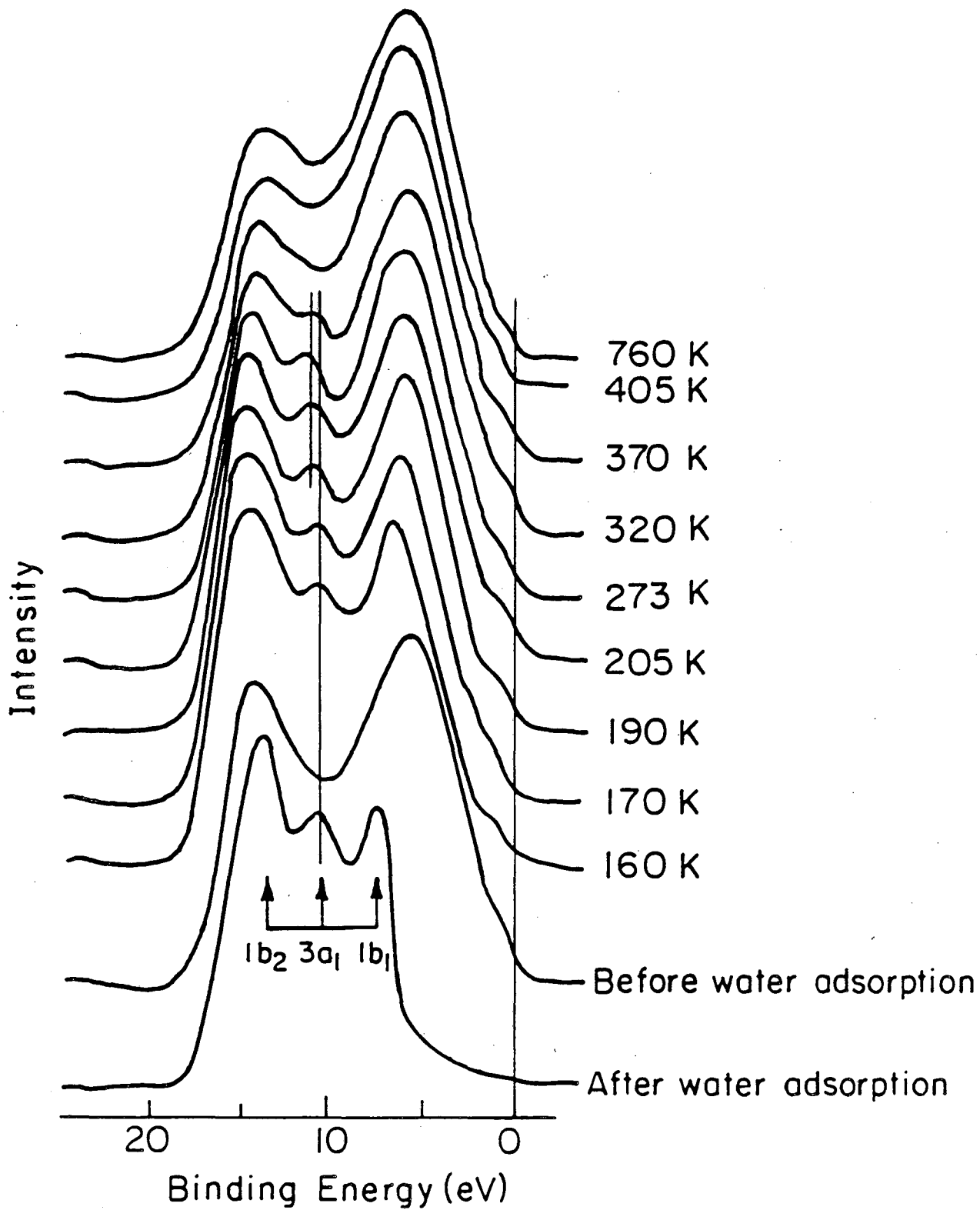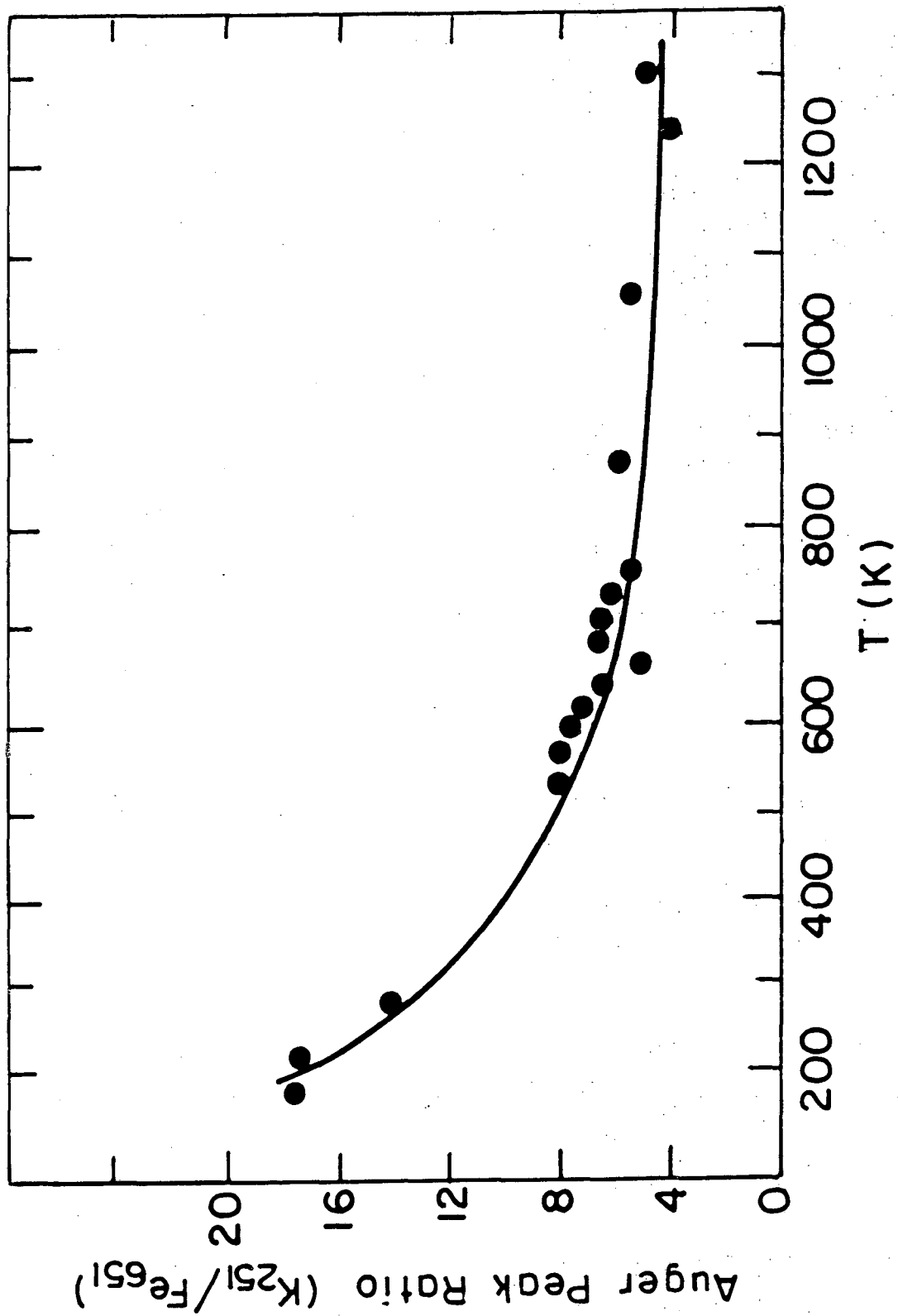
XBL 8511-4506

Fig. 10.

LAWRENCE BERKELEY LABORATORY
TECHNICAL INFORMATION DEPARTMENT
UNIVERSITY OF CALIFORNIA
BERKELEY, CALIFORNIA 94720